1992

Smooth Free-Form Surfaces over Irregular Meshes Generalizing quadratic splines

Jörg Peters

Report Number:
92-063

SMOOTH FREE-FORM SURFACES OVER IRREGULAR MESHES GENERALIZING QUADRATIC SPLINES

Jorg Peters

CSD-TR-92-063
September 22, 1992
(Revised 2/93)

Smooth free-form surfaces over irregular meshes generalizing quadratic splines

by

Jörg Peters[†]
jorg@cs.purdue.edu

Key words: C^1 surface, vertex enclosure, reparametrization, edge cutting, box splines, NURBS, blending

Running title: Smooth free-form surfaces over irregular meshes

Version: Feb 03 93 **Date printed:** February 4, 1993

Submitted to: Proceedings of the Oberwolfach conference June 1992, J. Hoschek (ed.)

Abstract

An algorithm for refining an essentially unrestricted mesh of points into a bivariate C^1 surface is given. The algorithm generalizes the construction of quadratic splines from a mesh of control points. It gives an explicit parametrization of the surface with quadratic and cubic pieces. When the mesh is regular then a quadratic spline surface is generated. Irregular input meshes with non quadrilateral mesh cells and more or fewer than four cells meeting at a point are allowed and generate spline spaces that generalize the space of quadratic splines. Consequently, the algorithm can model bivariate open or closed surfaces of arbitrary topological structure.

[†] Department of Computer Science, Purdue University, W-Lafayette IN 47907
Supported by NSF grant CCR-9211322

1. Introduction

B-splines are widely used to represent surfaces. They combine a low degree polynomial or rational representation of maximal smoothness with a geometrically intuitive variation of the surface in terms of the coefficients: by connecting the coefficients one obtains a mesh that roughly outlines the surface. Repeated refinement of this mesh by knot insertion results in a sequence of meshes whose points are averages of the preceding and whose limit is the surface itself. In addition to an elegant algebraic definition this yields an alternative geometric, procedural characterization of the splines useful for establishing many shape properties of spline surfaces. But the B-spline representation has a major shortcoming. It cannot model certain real world objects without singularity, because each point in the interior of the B-spline mesh must be *regular*, that is surrounded by exactly four quadrilateral mesh cells. This makes it impossible to choose for example the boundary mesh of a cube as input and in fact restricts the topological structure of the objects that can be modeled by the splines. Even if the object to be modeled can be described as a deformation of the plane, it may be more natural to have three or five quadrilaterals join at a point or to use non quadrilateral cells to model a feature. Using trimmed NURBS (non uniform rational B-splines) does not solve this problem since the trimming destroys one of the chief advantages of the B-spline representation, its built in smoothness. One ends up with the tricky task of smoothly joining the trimmed pieces. The goal of this and the earlier paper [Peters '92] is therefore to devise an algorithm that removes the regularity restrictions from the input mesh and yields a unified approach to surface modeling. The approach should reduce to the B-spline paradigm wherever the mesh is regular and have the following additional properties.

- There are no restrictions on the number of cells meeting at a mesh point or the number of edges to a mesh cell. Mesh cells need not be planar.
- The component functions of the spline surface form a vector space of smooth functions. In order to add and subtract the functions and locally edit the geometry, it suffices to add and subtract the mesh points locally.
- The surface is parametrized by low degree polynomial patches. The representation can be extended to rational patches.
- It is possible to interpolate the input mesh points and normals without solving a system of constraints.
- The coefficients of the parametrization can be obtained by applying averaging masks to the input mesh. Thus the algorithm can be interpreted as a rule for cutting an input polytope such that the limit polytope is the spline surface.
- The averaging or cutting process is geometrically intuitive. Smaller cuts result in a surface that follows the input mesh more closely and changes the normal direction more rapidly across the boundary.
- Cuts of zero depth result in a singular parametrization at the mesh points analogous to singularities of a quadratic spline with repeated knots. The C^1 surface degenerates into a C^0 surface that interpolates the edges of the input mesh and remains taut, e.g. planar when the mesh cell is planar.

In summary, one would like an algorithm that departs as little as possible from the NURB standard and combines the intuitive cutting paradigm with a low degree parametrization.

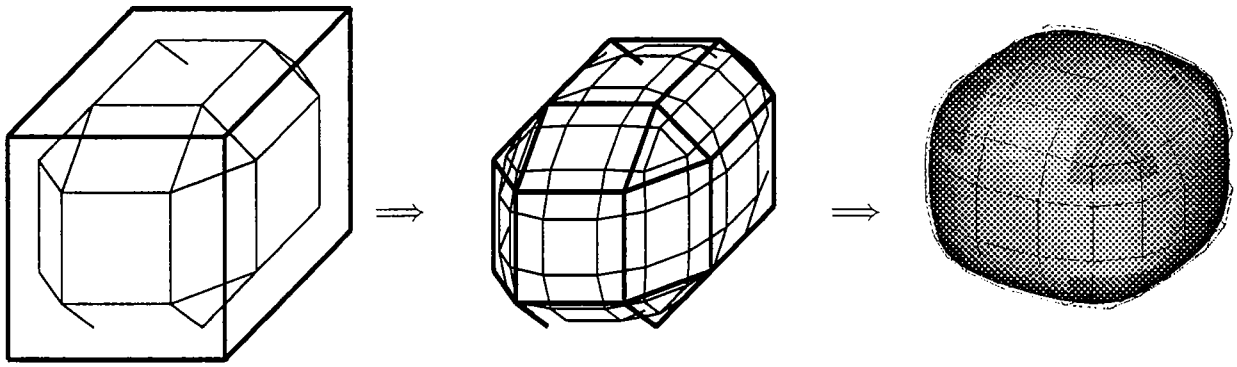

Figure 1.1: The cutting paradigm applied to a cube. The light regions of the output surface are covered by a quadratic spline, the dark regions by cubics.

The algorithm described in this paper generalizes the quadratic C^1 spline paradigm to generate surfaces with all the above properties. The central idea is to refine the irregular input mesh by a simple, linear averaging process and generate strips of regular mesh points that isolate regions of irregular points. Using this approach, [Peters '92] generates surfaces that consist of strips of biquadratic tensor-product splines complemented by bicubic patches to cover the isolated irregular mesh regions. The construction detailed in this paper uses the same cutting paradigm to generate the control points of quadratic box splines [1] and fills the holes with cubic triangular patches. Remarkably, filling in the cubics smoothly does not require solving systems of constraints. Rather, the cubics are determined by averaging the box spline control points such that, when applied to a hole with four edges, quadratic patches equivalent to the box spline surface are generated. The entire surface can be given a uniform representation in terms of triangular quadratic and cubic patches in Bernstein-Bézier form. The parametrization generated by the present algorithm is of lower total degree than the earlier tensor-product construction. While tensor product patches are to date more common, triangular patches have advantages when it comes to rendering.

The algorithm is in part motivated by algorithms for generalized subdivision ([Sabin '76], [Doo '78], [Catmull and Clark '78], [Loop '87], [Dyn, Levin and Liu '92], etc.). The algorithm does generalized subdivision. The main difference between the algorithm and earlier schemes is that the earlier schemes do not provide an explicit parametrization for the irregular mesh regions. This not only makes it tricky to establish elementary properties like tangent plane continuity of the limit surface, but is also a major obstacle for integrating these techniques with other CAGD representations. A second source of inspiration is the work on G-spline spaces by [Sabin '83], [Goodman '88] and [Höllig, Mögerle '89]. The present algorithm defines a G-spline space. The main difference between it and earlier approaches is that the present algorithm is more localized and does not need to solve large irregularly sparse systems of equations to match data. This makes it easier to reason

[1] Both the Bernstein-Bézier form and box splines are standard tools of geometric modeling. [Boehm, Farin, Kahmann '84] and [de Boor, Höllig, Riemenschneider 92] are good references. The quadratic box spline can be traced back to [Zwart '73] and [Powell '74].

about the shape of the resulting surface. A third foundation of the algorithm is the work on reparametrization and geometric smoothness (see e.g. [Gregory '90] for a survey). The algorithm of this paper differs from schemes like [Sarraga '87],[Hahn '89] in that no constraint systems have to be solved to enforce patch to patch smoothness. The vertex enclosure problem of joining surface pieces at a common point [Peters '91] is solved in a simple and natural fashion. While the present algorithm generates only tangent plane continuous surfaces, B-patches ([Seidel '91], [Dahmen, Micchelli, Seidel '9x]) offer kth order continuity for patches of degree $k+1$. However, currently B-patches are still slow to evaluate, suffer from a somewhat arbitrary choice of knots that influences the shape of the surface, and are, just like B-splines, restricted in their modeling capabilities. In comparison, the surfaces generated by the algorithm of this paper can be evaluated by subdivision, have intuitive cut ratios in lieu of knot spacings and can model arbitrary free-form objects. S-patches, as presented in [Loop, DeRose '90] require restricted input meshes. These restrictions can be removed by applying a Doo-Sabin refinement step or switching to the dual of the input mesh. The main drawback of the approach therefore seems to be the non standard representation and the slow evaluation of the rational surface pieces when the number of edges is large. Similar arguments apply to Gregory patches [Gregory '74].

The algorithm is detailed in Section 2. The end of Section 2 extends the algorithm to rational patches and interpolation of mesh vertices and rim curves. Section 3 establishes the continuity and vector space properties of the surfaces generated by the algorithm. Section 4 establishes the shape properties of the surfaces generated by the algorithm. Section 5 summarizes the findings and Section 6 gives three examples.

2. An algorithm for refining an irregular mesh of points into a C^1 surface

The three steps of the algorithm are:

- Refining the input mesh to generate the control points of the box spline surface.
- (Optional) Converting the box spline surface into Bernstein-Bézier form to make the representation uniform.
- Covering the remaining isolated holes with cubic patches.

The *input* is any mesh of points such that at most two cells abut along any edge. The mesh cells need not be planar, and there is no constraint on the number of edges to a cell or the number of cells meeting at a vertex. The mesh may model a bivariate open or closed surface of arbitrary topological structure. Each cell f of the input mesh has a shape parameter α_f, called *blend ratio*. The blend ratio is a number between zero and one. A smaller ratio results in a surface that follows the input mesh more closely and changes the normal direction more rapidly close to the mesh edges. The *output* of the algorithm are the Bernstein-Bézier coefficients of quadratic and cubic patches that parametrize a tangent-plane continuous surface. The surface interpolates the centroids of the cells of the input mesh. The *centroid* of a cell is defined as the average of its vertices.

1. Refining the input mesh to generate the control points of the box spline surface. We apply two steps of Doo-Sabin's averaging procedure [Doo '78]: at each step, s new points are created for each s-sided cell. Each new point connects to two new points generated at the two adjacent vertices of the same cell and the two adjacent cells of the same old mesh point. A new point corresponding to a vertex V of the cell f with centroid S has the coordinates

$$(1-\alpha_f)V + \alpha_f S$$

By default, the ratio of a cell in the second step is the average of the ratios of the old cells that contribute a vertex in the first step.

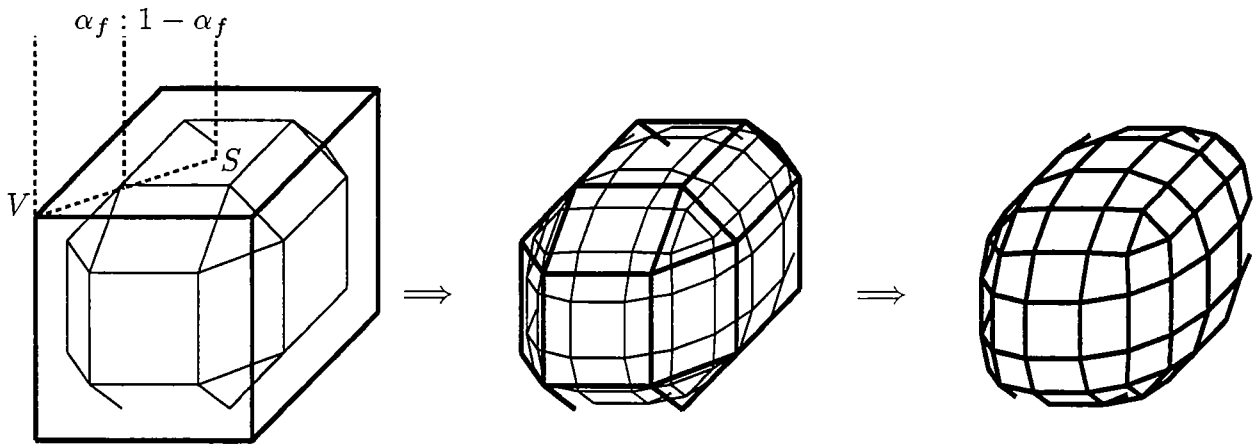

After refining the mesh, each mesh point is surrounded by four cells. If all four cells have exactly four edges, then the nine mesh points defining the cells can be interpreted as the control mesh of a box spline.

2. (Optional) Converting the box spline surface into Bernstein-Bézier form. This step may be omitted. It serves only to unify the surface representation in Bernstein-Bézier form. By symmetry it suffices to give the conversion formula for the following four Bernstein-Bézier coefficients in terms of the box spline control points.

$$Q_{002} = \frac{1}{8}(C_1 + C_2 + C_3 + C_4 + 4A)$$
$$Q_{011} = \frac{1}{8}(2C_2 + 2C_3 + 4A)$$
$$Q_{020} = \frac{1}{8}(2C_2 + 2C_3 + 2A + 2B_2)$$
$$Q_{110} = \frac{1}{8}(4C_2 + 4A)$$

Since Q_{020} is both the centroid of a quadrilateral mesh cell and a vertex Bernstein-Bézier coefficient, the centroids of the cells are interpolated.

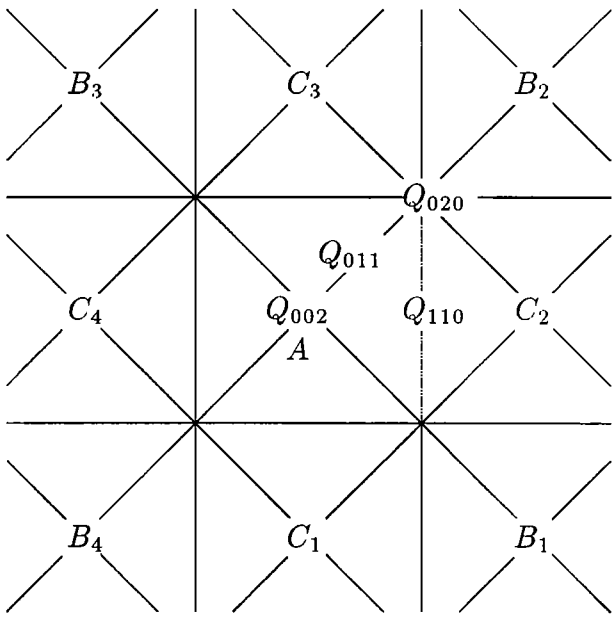

Figure 2.1: Transforming the box spline control mesh with points A, B_i, C_i into a mesh of Bézier coefficients Q_{ijk}.

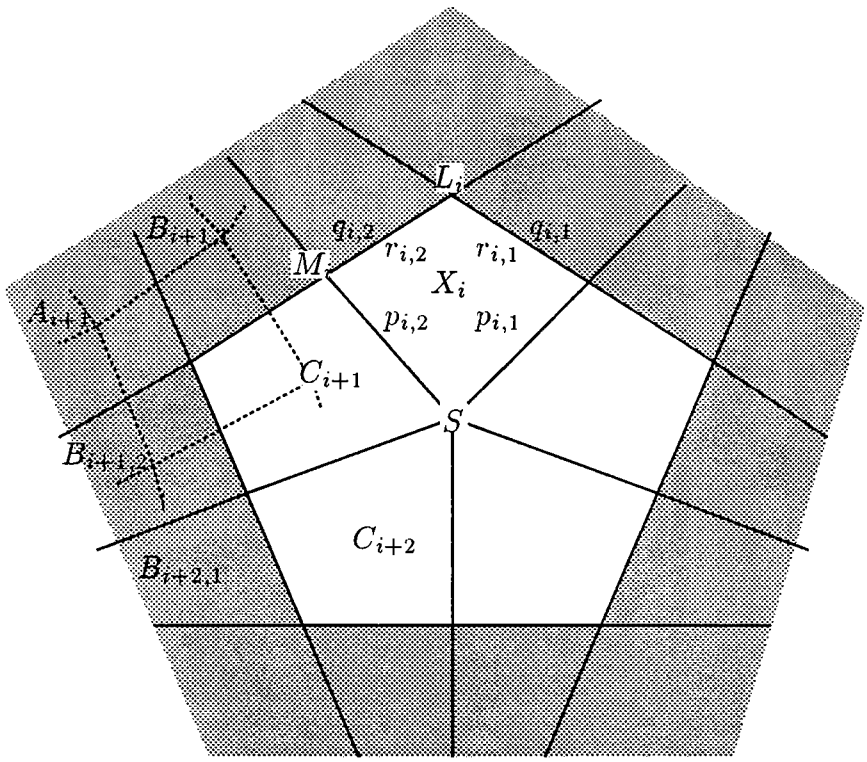

Figure 2.2: Each quadrilateral of the 5-sided cell is covered by 4 triangular patches: $r_{i,1}$, $p_{i,1}$, $p_{i,2}$, $r_{i,2}$. – A_i, B_{ij}, C_i are box spline control points as in Figure 2.1.

3. Covering the remaining isolated holes with cubic patches. Each non quadrilateral, s-sided mesh cell is divided into quadrilaterals $i = 1..s$ each of which is covered by four triangular patches, p_{ij} and r_{ij}, $j = 1, 2$, with Bernstein-Bézier coefficients $P_{klm,ij}$, and $R_{klm,ij}$. If Step 2 is executed, then the cell is surrounded by $2s$ patches $q_{i,j}$ with coefficients $Q_{klm,ij}$ as shown in Figure 2.3. First one determines S, the centroid of the mesh cell and various auxiliary vectors:

$$S := \frac{1}{s}\sum_{i=1}^{s} C_i, \qquad E_i := \frac{C_i + C_{i+1}}{2}, \qquad M_i := \frac{C_i + C_{i+1} + B_{i+1,1} + B_{i,2}}{4},$$

$$F_{i,j} := \frac{C_i + B_{i,j}}{2}, \qquad L_i := \frac{C_i + B_{i,1} + B_{i,2} + A_i}{4}.$$

The boundary curves of the cell are degree raised quadratics:

$$R_{030,i2} = L_i, \quad R_{120,i2} = \frac{1}{3}(L_i + 2F_{i,2}), \quad R_{210,i2} = \frac{1}{3}(M_i + 2F_{i,2}), \quad R_{300,i2} = M_i.$$

The tangent coefficient P_{210} is chosen by extending the box spline.

$$P_{210,i2} = \frac{2}{3}E_i + \frac{1}{3}M_i.$$

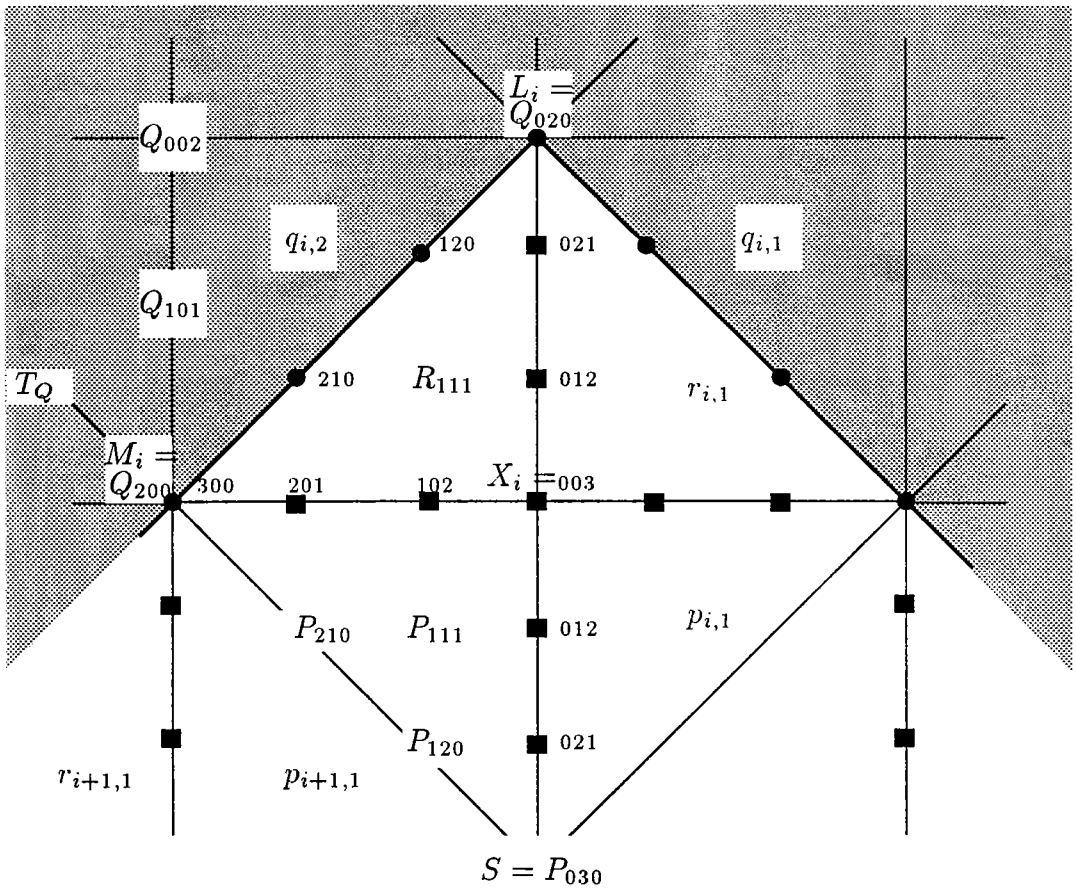

Figure 2.3: Enlargement of the corner L_i.
The cubic construction consists mainly of degree-raising (•) and averaging (■).
$R_{111} = R_{111,i,2}$, $P_{111} = P_{111,i,2}$, $P_{210} = P_{210,i,2}$, $P_{120} = P_{120,i,2}$.

The tangents of the curves M_iX_i and L_iX_i are computed as averages weighed by $c := \cos(\frac{\pi}{s})$:

$$R_{201,ij} = c^2 R_{210,ij} + (1-c^2)P_{210,ij}, \quad R_{021,ij} = \frac{1}{2}R_{120,i2} + \frac{1}{2}R_{120,i1}, \text{ and}$$

$$R_{111,i2} = R_{120,i2} + \frac{1}{12}(C_{i+1} - B_{i,2} + 2(1-c^2)(C_i - A_i)).$$

The tangent coefficients $P_{120,i}$ at S are generated by applying a discrete first order Fourier filter as in [Loop '90, Fig.3], [Van Wijk '86 (14)]:

$$P_{120,ij} = S + \alpha \sum_{l=1}^{s} \cos(\frac{2\pi}{s}l)E_{i+l}.$$

Here $\alpha \in (0,1)$ is the shape parameter of the cell analogous to the blend ratio in the mesh

refinement; $\alpha = \frac{4}{3s}$ is the recommended value. Finally,

$$
\begin{aligned}
R_{021,i2} &= R_{021,i1} = \frac{1}{2}R_{111,i2} + \frac{1}{2}R_{111,i1},\\
P_{021,i2} &= P_{021,i1} = \frac{1}{2}P_{120,i2} + \frac{1}{2}P_{120,i1},\\
P_{111,i2} &= (1-c^2)P_{120,i2} + c^2P_{210,i2} + \frac{1}{4}(P_{201,i2} - P_{201,i+1,1} + P_{021,i2} - P_{021,i+1,1}),\\
P_{012,i2} &= P_{012.i1} = \frac{1}{2}P_{111,i2} + \frac{1}{2}P_{111,i1},\\
P_{102,i2} &= R_{102.i2} = (1-c^2)P_{111,i2} + c^2R_{111,i2},\\
P_{003,i2} &= P_{003,i1} = R_{003,i2} = R_{003,i1} = \frac{1}{2}P_{102,i2} + \frac{1}{2}P_{102,i1}.
\end{aligned}
$$

By symmetry, this determines all the coefficients of the cubic patches, e.g. $P_{111,i1} = (1 - c^2)P_{120,i1} + c^2P_{210,i1} + \frac{1}{4}(P_{201,i1} - P_{201,i-1,2} + P_{021,i1} - P_{021,i-1,2})$.

Extensions of the Algorithm:

- A different combination of blend ratios can be used in each step and the blend ratios may be individually changed and associated with edges rather than with cells. The above choice is just a default to simplify the exposition.
- A vertex V of the input mesh can be interpolated as follows. After the first of the two refinement steps, move the points P_i, $i = 1..s$ of the refined mesh constructed around V by $V - \frac{1}{s}\sum_{i=1}^{s} P_i$. Then V is the centroid of the resulting cell and will be interpolated by Proposition 3.5. Similarly, one can interpolate normals at the vertices. The approach must be used cautiously since it extrapolates and hence may create additional features on the surface.
- To obtain rational surfaces, one simply associates a fourth coordinate with each box spline control point and applies the algorithm to points in $\mathbb{R}^4$. The fourth coordinate corresponds to the coefficient of the rational weight function (cf. Corollary 3.3).
- Like purely B-spline based splines, an open surface shrinks away from the rim of its input mesh. Its rim curve is by default piecewise quadratic. A piecewise curve that closely follows the outlines of the original input mesh rim can be interpolated with the following ad hoc measure. Extend the boundary patches by reflection, and replace the outermost layer of coefficients of the extrapolated patches with the coefficients of the piecewise curve. Then average the coefficients second layer of coefficients from the rim to smooth out the result.

3. Continuity and vector space properties

This section shows that splines generated by the surface form a smooth vector space. Smoothness, oriented tangent plane continuity is characterized as the agreement of the derivatives of two maps p and q from $\mathbb{R}^2$ to $\mathbb{R}^n$ after reparametrization by a map φ from $\mathbb{R}^2$ to $\mathbb{R}^2$ that connects the domains Ω_p and Ω_q of p and q:

$$p = q \circ \varphi \quad \text{and} \quad D_1 p = D_1(q \circ \varphi) \quad \text{along } E_p$$

where $\varphi(E_p) = E_q$, E_p and E_q are edges of Ω_p and Ω_q respectively. D_1 denotes differentiation in the direction perpendicular to E_p and φ maps interior points of Ω_q to exterior points of Ω_p to avoid cusps. We prepare the result with the following lemma.

(3.1) Lemma. *The choice of the coefficients P_{111} minimizes the deviation from the center coefficient of a degree-raised quadratic subject to the continuity constraints.*

Proof Define P^*_{111} as the central coefficient of a degree-raised quadratic based on given boundary data in Step 3 of the algorithm:

$$P^*_{111} := \frac{1}{4}(2P_{201} + 2P_{021} + P_{120} + P_{210} - P_{300} - P_{030}).$$

The expression for P_{111} minimizes $(P_{111,i,1} - P^*_{111,i,1})^2 + (P_{111,i,2} - P^*_{111,i,2})^2$ subject to the C^1 constraint $\frac{1}{2}P_{111,i+1,1} + \frac{1}{2}P_{111,i,2} = (1-c^2)P_{120,i,2} + c^2 P_{210,i,2}$. By Lagrangian duality, this minimization problem is solved by

$$P_{111,i,2} = (1-c^2)P_{120,i,2} + c^2 P_{210,i,2} + \frac{1}{2}(P^*_{111,i,2} - P^*_{111,i+1,1})$$

as claimed. ■

(3.2) Theorem. *The surface constructed by the algorithm in Section 2 is C^1.*

Proof With $c := \cos(\frac{\pi}{s})$. and $a := \frac{c^2}{1-c^2}$, the transitions between the patches are as follows (cf. Figure 2.2).
(1) Across the edges L_iM_i, $r_{i,j}$ is constructed by enforcing $r_{i,j}(E_j) = q_{i,j}(\phi_{i,j}(E_j))$ and $D_j r_{i,j} = D_j(q_{i,j} \circ \phi_{i,j})$, where t_1 parametrizes the edge L_iM_i, t_2 the edge L_iM_{i-1} and

$$\phi_{i,1} := \mathrm{id} + t_1 t_2 \begin{bmatrix} 1-2c^2 \\ 0 \end{bmatrix}, \quad \phi_{i,2} := \mathrm{id} + t_1 t_2 \begin{bmatrix} 0 \\ 1-2c^2 \end{bmatrix}.$$

(2) Across the edges M_iS, $D_1 p_{i,2} = D_1(p_{i+1,1} \circ \psi_i)$, where t_1 parametrizes the edge M_iL_{i+1}, t_2 the edge M_iS and

$$\psi_i := \mathrm{id} + t_1 \begin{bmatrix} 0 \\ 1-2c^2 \end{bmatrix}.$$

(3) Across the edges L_iX_i and X_iS, the reparametrization is the identity and (4) across the edges M_iX_i and $M_{i-1}X_i$, it is the scaling $\mathrm{id}^a := a * \mathrm{id}$. Due to the simplicity of the maps

(3) and (4), we may concentrate on the construction of P_{210}, R_{111}, P_{111} and P_{120}. Writing $[b_0,\ldots,b_d]$ for $p : t \mapsto \sum_{j=0}^{d} t^j(1-t)^{d-j}b_j$, the C^1 constraints $D_2 r_{i,2} = D_2(q_{i,2} \circ \phi_{i,2})$, across L_iM_i in Bernstein-Bézier form are

$$2[1,\ell][Q_{110}-Q_{020}, Q_{200}-Q_{110}] =$$

$$3[R_{021}-R_{030}, 2(R_{111}-R_{120}), R_{201}-R_{210}] + 2[1,m][Q_{011}-Q_{020}, Q_{101}-Q_{110}],$$

where $Q_{200,i2} = M_i$, $Q_{101,i2} = (2B_{i,2}+C_i+B_{i+1,1})/4$, $Q_{011,i2} = (2B_{i,2}+C_i+A_i)/4$, and $Q_{110,i2} = F_{i2}$. Since $Q_{101}-Q_{110} = \frac{T_Q-Q_{110}}{2}$, $T_Q := (B_{i,2}+B_{i+1,1})/2$ and $R_{201}-R_{210} = \frac{2}{3}(P_{210}-R_{210})(1-c^2) = \frac{2}{3}(-T_Q-Q_{110})(1-c^2)$ and since $T_Q - M$ and $Q_{110}-M$ are in general linearly independent, the third equation,

$$2\ell(M-Q_{110}-M) = m(T_Q-Q_{110}) + 2(-T_Q-Q_{110})(1-c^2),$$

implies $\ell = m = 2(1-c^2)$. Therefore the second constraint is

$$R_{111} = R_{120} + \frac{1}{3}(Q_{200}-Q_{110}-(Q_{101}-Q_{110}) + \ell(Q_{110}-Q_{020}-(Q_{011}-Q_{020}))).$$

This is enforced by the construction.

Setting $S=0$, the coplanarity of the tangent coefficients P_{120} at S follows from

$$\sum_{i=1}^{s} \cos(\frac{2\pi}{s}i)(P_{120,i-1} - 2cP_{120,i} + P_{120,i+1})$$
$$= \sum_{i=1}^{s} P_{120,i}\big(\cos(\frac{2\pi}{s}(i-1)) + \cos(\frac{2\pi}{s}(i+1)) - 2\cos(\frac{2\pi}{s})\cos(\frac{2\pi}{s}i)\big) = 0.$$

The choice of P_{111} in Lemma 3.1 enforces the remaining constraint $D_1 p_{i,2} = D_1(p_{i+1,1} \circ \psi_i)$ across the edges M_iS:

$$\begin{aligned} 2(1-c^2)&[P_{210,i,2}-P_{300,i,2}, 2(P_{120,i,2}-P_{210,i,2}), P_{030,i,2}-P_{120,i,2}] \\ &= [P_{201,i,2}-P_{300,i,2}, 2(P_{120,i,2}-P_{210,i,2}), P_{021,i,2}-P_{120,i,2}] \\ &+ [P_{201,i+1,1}-P_{300,i+1,1}, 2(P_{120,i+1,1}-P_{210,i+1,1}), P_{021,i+1,1}-P_{120,i+1,1}]. \end{aligned}$$

■

(3.3) Corollary. *The rational surface generated by applying the algorithm to vectors with four components and using the last component as the coefficient of the denominator is tangent plane continuous when the denominator does not vanish.*

Proof If $P, Q : [0..1]^2 \mapsto \mathbb{R}^3$ and $p, q : [0..1]^2 \mapsto \mathbb{R}$ and $P = Q$ and $p = q \neq 0$ along a boundary shared by the functions P/p and Q/q, then

$$D_1(\frac{P}{p}) = D_1(\frac{Q}{q} \circ \phi) \quad \Longleftrightarrow \quad q(D_1P - D_1(Q \circ \phi)) = Q(D_1 p - D_1(q \circ \phi))$$

along that boundary. When the algorithm is applied to the coefficients of $(P,p) \in \mathbb{R}^4$, then the second factor on either side of the equation vanishes and hence the transition is tangent plane continuous. ■

An important property of splines is that they form a vector space. In particular, it suffices to add and subtract the control meshes in order to add and subtract the corresponding surface provided the knot spacing agrees. For the spline surfaces generated by the present algorithm the role of the knot distances is played by the blend ratios.

(3.4) Theorem. *C^1 surfaces generated from input meshes with the same connectivity and the same blend ratio for corresponding cells form a vector space.*

Proof Trivially, if $P = \sum \alpha_i P_i$ and $Q = \sum \alpha_i Q_i$ are are points of the refined mesh constructed with the same blend ratios α_i, then $P + Q = \sum \alpha_i (P_i + Q_i)$ as the additive vector space property requires. Two surfaces generated from input meshes with the same connectivity have a natural 1-1 and onto correspondence of patches. Consider two smoothly abutting patches p_i and q_i, $i = 1,2$ of the ith surface. The connecting map depends only on the connectivity of the mesh via c. Identifying the open neighborhood of the edges $E_{p,1}$ and $E_{p,2}$ as E_p, there is a single connecting map φ such that

$$p_i = (q_i \circ \varphi) \quad \text{and} \quad D_1 p_i = D_1(q_i \circ \varphi) \quad \text{along } E_p.$$

Consequently, if $p_0 := \beta_1 p_1 + \beta_2 p_2$ and $q_0 := \beta_1 q_1 + \beta_2 q_2$, then

$$p_0 = (q_0 \circ \varphi) \quad \text{and} \quad D_1 p_0 = D_1(\beta_1 p_1 + \beta_2 p_2) = \beta_1 q_1 \circ \varphi + \beta_2 q_2 \circ \varphi = D_1(q_0 \circ \varphi)$$

along E_p as claimed. ■

Since the refinement and patch construction consists of linear operations, it commutes with affine operators. To model with the vector space it is good to know that the resulting surfaces interpolate averages of the input mesh points.

(3.5) Proposition. *The surface generated by the algorithm interpolates the centroids of the cells of the input mesh.*

Proof In the regular control mesh regions, the coefficients Q_{020} generated in Step 2 of the algorithm are both the centroid of a quadrilateral mesh cell and a vertex Bernstein-Bézier coefficient. In the regular control mesh regions, Step 3 explicitly chooses the centroid to be the vertex Bernstein-Bézier coefficient S. ■

4. Shape properties of the resulting surface

Symmetry and regularity of the input mesh lead to a a simpler parametrization. This is the theme of the first two propositions. A third proof of this section establishes that the surfaces are flat in the neighborhood of the image of a mesh point if and only if the mesh is locally flat. Finally, we show that the edges of the input mesh are interpolated and thus the outlines of the input polytope recaptured when the blend ratios are zero.

When the number of edges of the mesh cell covered in Step 3 of the algorithm is $s = 4$, then $c = \sqrt{2}/2$ and hence $a = 1$ and $1 - 2c^2 = 0$. That is, all connecting maps become the identity at a regular mesh point. This motivates the next two proofs.

(4.1) Proposition. *If the control points C_i of a mesh cell form an affine s-gon, then the boundary curves M_iS are quadratic.*

Proof Let $L^{-1} * C_i$ be the vertices of a regular s-gon. Then $P_{210} = M_i + \frac{2}{3}(E_i - M_i)$ and $P_{120} = \frac{2}{3}L * \frac{L^{-1}C_i + L^{-1}C_{i+1}}{2} \frac{2}{s} \sum \cos^2(\frac{2\pi}{s} l) = \frac{2}{3}E_i$ are identical to the coefficients of the degree raised quadratic with coefficients M_i, E_i and $S = 0$. ■

(4.2) Proposition. *If Step 3 of the algorithm is applied to a 4-sided mesh hole, then the patches generated are quadratic.*

Proof If $s = 4$, then $\phi_{i,j} = \psi_i = \mathrm{id}^a = \mathrm{id}$. Since $P_{120,i} = S + \frac{2}{3}(\frac{C_i + C_{i+1}}{2} - S)$, the boundary curve M_iS is a quadratic with coefficients M_i, E_i and S. Rewriting the expressions in terms of the control points A_i, $B_{i,1}$, $B_{i,2}$ and C_i shows that

$$\frac{E_i + Q_{110,i,2}}{2} = R^*_{101} := Q_{200} + (Q_{110} - Q_{101})$$
$$\frac{Q_{110,i,2} + Q_{110,i,1}}{2} = R^*_{011} := Q_{020} + (Q_{110} - Q_{011})$$

Set $R^*_{110} := Q_{110}$, then

$$R_{111} = \frac{1}{3}(Q_{110} + Q_{200} + (Q_{110} - Q_{101}) + Q_{020} + (Q_{110} - Q_{011}))$$

is the center coefficient of a degree-raised quadratic patch r^*. Similarly one checks that

$$P_{111,i,2} = \frac{1}{2}P_{120,i,2} + \frac{1}{2}P_{210,i,2} + \frac{1}{4}(P_{201,i,2} - P_{201,i+1,1} + P_{021,i,2} - P_{021,i+1,1})$$

is the center coefficient of a degree-raised quadratic patch p^* with boundary coefficients $P^*_{110} := E_i$, $P^*_{011} := \frac{E_i + E_{i-1}}{2}$ and $P^*_{101} := R^*_{101}$. Since the remaining coefficients corresponding to the curves emanating from X_i are computed by averaging, the result follows. ■

Another special geometric configuration simplifies the box spline surface. In the notation of Figure 2.1, the four triangular patches around A are a single quadratic if and only if $B_i - (C_i + C_{i+1}) = B_{i+2} - (C_{i+2} + C_{i+3})$ for $i = 1$ and $i = 2$ counting modulo four since this forces a C^2 connection between the quadratic patches. Next, we turn to the curvature at the join of patches. If two consecutive layers of coefficients lie in the same plane, then the surface is locally planar.

(4.3) Proposition. *The curvature at S is zero if and only if $P_{210,i}, i = 1..s$ and S lie in the same plane.*

Proof All $P_{120,i}$ and S lie in the same tangent plane with normal direction $n = F_i \times F_{i+1}$, where $F_i := \sum_{l=1}^{s} \cos(\frac{2\pi}{s} l) P_{210,l+i}$. Let $P(n)$ be the component of P normal to the tangent plane. If some $P_{210,i}$ does not lie in that plane, then (a) the curvature of the ith boundary curve is nonzero and (b) the $P_{111,i}$ do not all lie in the plane since $P_{111}(n) = c^2 P_{210}(n)$. Conversely, if all $P_{210,i}$ lie in the tangent plane, then the normal components of all $P_{111,i}$ are zero. ■

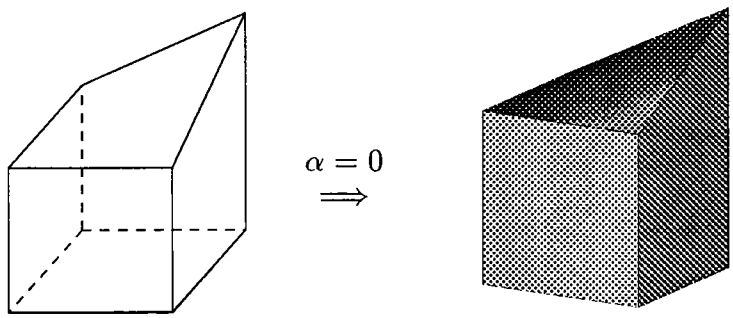

Figure 4.4: Zero blend ratios induce a C^0 surface that tightly interpolates the input mesh: a cube with the $(1,1,1)$-vertex replaced by $(1,1,2)$.

Zero cut ratios result is a singular parametrization at the input mesh point analogous to singularities in B-spline based curves or surface with coalesced knots. This has the desirable consequence that the C^1 surface degenerates into a C^0 surface that tightly interpolates the input mesh.

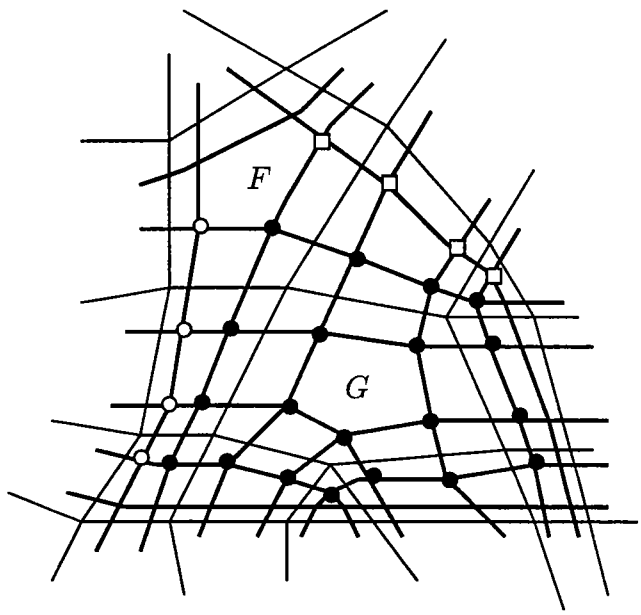

Figure 4.5: Zero blend ratios coalesce all control points • into the input mesh point G.